

# Non-contact sub-nanometer optical repositioning using femtosecond lasers

Yves Bellouard

Galatea Lab, STI/IMT, Ecole Polytechnique Fédérale de Lausanne (EPFL), Neuchâtel, Switzerland  
[yves@bellouard.eu](mailto:yves@bellouard.eu)

**Abstract:** Optical components like resonator or waveguides often have stringent requirements in term of positioning accuracy during packaging. While this can be done routinely in a laboratory environment, permanently positioning and aligning optical elements with nanometer accuracy in a fully packaged device is a challenging endeavor. Here, we demonstrate the use of femtosecond laser-induced modifications in glass for the remote permanent fine-positioning of an optical element with sub-nanometer resolution.

©2015 Optical Society of America

**OCIS codes:** (140.3390) Laser materials processing; (160.6030) Silica; (320.2250) Femtosecond phenomena;

---

## References and Links

1. W. H. F. Andreasch, "Konzeption und Entwicklung einer Technologie zur automatisierten Oberflächenmontage optischer Elemente (optical SMD)," Ph.D. Thesis, EPFL, n° 1591 (1996).
2. M. Scussat, "Assemblage bidimensionnel de composants optiques miniatures," Ph.D. Thesis, EPFL, n° 2179 (2001).
3. W. Hoving, "Accurate manipulation using laser technology," Proc. SPIE **3097**, 284–295 (1997).
4. M. Leers, M. Winzen, E. Liermann, H. Faidel, T. Westphalen, J. Miesner, J. Luttmann, and D. Hoffmann, "Highly precise and robust packaging of optical components," Proc. SPIE **8244**, 824404 (2012).
5. Y.-C. Hsu, "Novel butterfly type laser module packaging," J. Laser Micro/Nanoeng. **6**(3), 255–258 (2011).
6. M. Geiger and F. Meyer-Pittroff, "Laser beam bending of metallic foils," Proc. SPIE **4426**, 187–190 (2002).
7. S. A. Diamond, "Active-Core-Alignment," <http://www.diamond-fo.com/technologies/Active-Core-Alignment-A-C-A.html>
8. J. H. C. van Zantvoort, G.-D. Khoe, and H. D. Waardt, "Fiber array-to-photonics-chip fixation and fine tuning using laser support adjustment," IEEE J. Sel. Top. Quant. **8**(6), 1331–1340 (2002).
9. J. H. C. van Zantvoort, S. G. L. Plukker, E. C. A. Dekkers, G. D. Khoe, A. M. J. Koonen, and H. de Waardt, "Integration of laser-support fiber adjustment in opto-electronic modules," in Electronics System-Integration Technology Conference, 2008. ESTC 2008. 2nd (IEEE, 2008), pp. 803–808.
10. J. H. C. Van Zantvoort, S. G. L. Plukker, E. C. A. Dekkers, G. D. Petkov, G. D. Khoe, A. M. J. Koonen, and H. Waardt, "Lensed fiber-array assembly with individual fiber fine positioning in the submicrometer range," IEEE J. Sel. Top. Quantum Electron. **12**(5), 931–939 (2006).
11. J. H. Song, H. N. J. Fernando, B. Roycroft, B. Corbett, and F. H. Peters, "Practical design of lensed fibers for semiconductor laser packaging using laser welding technique," J. Lightwave Technol. **27**(11), 1533–1539 (2009).
12. H. Shen, X. Wang, and W. Qiang, "Online postwelding shift compensation in butterfly laser module packages based on welding spot distance," Opt. Eng. **48**(12), 124301 (2009).
13. Z. Shen, C. Gu, H. Liu, and X. Wang, "An experimental study of overlapping laser shock micro-adjustment using a pulsed Nd:YAG laser," Opt. Laser Technol. **54**, 110–119 (2013).
14. Y. Bellouard, A. Said, and P. Bado, "Integrating optics and micro-mechanics in a single substrate: a step toward monolithic integration in fused silica," Opt. Express **13**(17), 6635–6644 (2005).
15. Y. Bellouard, "On the bending strength of fused silica flexures fabricated by ultrafast lasers [Invited]," Opt. Mater. Express **1**(5), 816–831 (2011).
16. V. Tielen and Y. Bellouard, "Three-dimensional glass monolithic micro-flexure fabricated by femtosecond laser exposure and chemical etching," Micromachines (Basel) **5**(3), 697–710 (2014).
17. A. Marcinkevičius, S. Juodkazis, M. Watanabe, M. Miwa, S. Matsuo, H. Misawa, and J. Nishii, "Femtosecond laser-assisted three-dimensional microfabrication in silica," Opt. Lett. **26**(5), 277–279 (2001).
18. S. Kiyama, S. Matsuo, S. Hashimoto, and Y. Morihira, "Examination of etching agent and etching mechanism on femtosecond laser microfabrication of channels inside vitreous silica substrates," J. Phys. Chem. C **113**(27), 11560–11566 (2009).

19. A. Champion and Y. Bellouard, "Direct volume variation measurements in fused silica specimens exposed to femtosecond laser," *Opt. Mater. Express* **2**(6), 789–798 (2012).
20. Y. Bellouard, T. Colomb, C. Depeursinge, M. Dugan, A. A. Said, and P. Bado, "Nanoindentation and birefringence measurements on fused silica specimen exposed to low-energy femtosecond pulses," *Opt. Express* **14**(18), 8360–8366 (2006).
21. A. Champion, M. Beresna, P. Kazansky, and Y. Bellouard, "Stress distribution around femtosecond laser affected zones: effect of nanogratings orientation," *Opt. Express* **21**(21), 24942–24951 (2013).
22. B. McMillen and Y. Bellouard, "On the anisotropy of stress-distribution induced in glasses and crystals by non-ablative femtosecond laser exposure," *Opt. Express* **23**(1), 86–100 (2015).
23. P. S. Salter and M. J. Booth, "Focussing over the edge: adaptive subsurface laser fabrication up to the sample face," *Opt. Express* **20**(18), 19978–19989 (2012).
24. S. Hasegawa and Y. Hayasaki, "Holographic vector wave femtosecond laser processing," *Int. J. Optomech.* **8**(2), 73–88 (2014).
25. Y. Bellouard, A. Said, M. Dugan, and P. Bado, "Fabrication of high-aspect ratio, micro-fluidic channels and tunnels using femtosecond laser pulses and chemical etching," *Opt. Express* **12**(10), 2120–2129 (2004).
26. J. Squier, M. Muller, G. Brakenhoff, and K. R. Wilson, "Third harmonic generation microscopy," *Opt. Express* **3**(9), 315–324 (1998).
27. Y. Barad, H. Eisenberg, M. Horowitz, and Y. Silberberg, "Nonlinear scanning laser microscopy by third harmonic generation," *Appl. Phys. Lett.* **70**(8), 922 (1997).
28. M. Müller, J. Squier, K. R. Wilson, and G. J. Brakenhoff, "3D microscopy of transparent objects using third-harmonic generation," *J. Microsc.* **191**(3), 266–274 (1998).
29. J. A. Squier and M. Müller, "Third-harmonic generation imaging of laser-induced breakdown in glass," *Appl. Opt.* **38**(27), 5789–5794 (1999).
30. C. B. Schaffer, J. Aus der Au, E. Mazur, and J. A. Squier, "Micromachining and material change characterization using femtosecond laser oscillators," *Proc. SPIE* **4633**, 112–118 (2002).
31. K. M. Davis, K. Miura, N. Sugimoto, and K. Hirao, "Writing waveguides in glass with a femtosecond laser," *Opt. Lett.* **21**(21), 1729–1731 (1996).
32. K. Minoshima, A. M. Kowalevich, I. Hartl, E. P. Ippen, and J. G. Fujimoto, "Photonic device fabrication in glass by use of nonlinear materials processing with a femtosecond laser oscillator," *Opt. Lett.* **26**(19), 1516–1518 (2001).
33. S. Nolte, M. Will, J. Burghoff, and A. Tuennermann, "Femtosecond waveguide writing: a new avenue to three-dimensional integrated optics," *Appl. Phys. A – Mater.* **77**(1), 109–111 (2003).
34. G. D. Marshall, R. J. Williams, N. Jovanovic, M. J. Steel, and M. J. Withford, "Point-by-point written fiber-Bragg gratings and their application in complex grating designs," *Opt. Express* **18**(19), 19844–19859 (2010).
35. V. Maselli, J. R. Grenier, S. Ho, and P. R. Herman, "Femtosecond laser written optofluidic sensor: Bragg grating waveguide evanescent probing of microfluidic channel," *Opt. Express* **17**(14), 11719–11729 (2009).
36. E. Bricchi, J. D. Mills, P. G. Kazansky, B. G. Klappauf, and J. J. Baumberg, "Birefringent Fresnel zone plates in silica fabricated by femtosecond laser machining," *Opt. Lett.* **27**(24), 2200–2202 (2002).
37. J. Drs, T. Kishi, and Y. Bellouard, "Laser-assisted morphing of complex three dimensional objects," *Opt. Express* **23**(13), 17355–17366 (2015).
38. J. Tang, J. Lin, J. Song, Z. Fang, M. Wang, Y. Liao, L. Qiao, and Y. Cheng, "On-chip tuning of the resonant wavelength in a high-Q microresonator integrated with a microheater," *I. J. Optomech.* **9**(2), 187–194 (2015).

## 1. Introduction

A variety of optical phenomena are highly sensitive to position fluctuations and fine alignments. While this can be advantageously used for sensing displacements in the nanometer range, it also represents a formidable challenge when it comes to packaging optical elements of different nature and assembling them together, so that the integrity of the device function is maintained. Typical examples among others are the coupling between optical waveguides, the alignment between whispering gallery modes (WGM) resonators and waveguides, miniaturized interferometric systems. Packaging operations eventually require the use of permanent attaching methods like welding, bonding or soldering that inherently create distortions in initially perfectly aligned devices. This is a well-known issue in the production of optical devices in particular.

To address the challenge of maintaining high precision alignment in final products, various strategies have been proposed. One first intuitive approach consists in pre-compensating for post-attachment shifts like post-weld or post-bonding shifts (see for instance [1–5]). A second one is to correct for misalignment and post-assembly distortions by locally deforming the material supporting the optical components [6]. This second approach has been implemented using mechanical deformation (for instance using an indenter-like tool to

reposition the core of an optical fiber within a concentric reference in high-end fiber connectors [7]), or using localized surface laser-melted spots (see refs [8–13], as examples for various optical components). There, the working principle is to use rapid heat-driven volume-change to locally and plastically deform a supported structure, in order to achieve permanent deformations.

Both strategies suffer from intrinsic limitations. The first one – i.e. the pre-compensation scheme, requires not only an accurate knowledge of the post-attachment shifts, but also requires these shifts to be highly repeatable and not prone to variability. The process tolerances will therefore define the achievable positioning accuracy. The second one – i.e. localized mechanical deformation, requires a mechanical contact with the element to be repositioned, which may not be accessible and is limited to specific geometries. Finally, the use of laser-melt spot to plastically deform objects suppresses the need for direct mechanical contact, but only works on absorbent and plastically deformable substrates. Since it is based on a classical absorption mechanism, the laser only interacts with a surface layer on the structure which dramatically limits repositioning capabilities and put severe constraints on the supporting element geometry.

Here we propose to use non-linear matter interaction to induce localized volume changes in the bulk of transparent optical-mount elements. These volume changes can be controlled accurately and arranged spatially with a specific strategy to induce a prescribed motion of the element to be repositioned. Furthermore, and to achieve precise and controlled displacements along the geometrical axis defining the orientation of the device, the laser-induced volume expansion can be combined with advanced mechanical elements such as flexures to form complex kinematics able to produce controlled motions. In this paper, to illustrate the feasibility of this concept, we present a one-axis glass kinematics being repositioned with sub-nanometer accuracy. As it will be seen later on, this concept can be extended to virtually any degree of freedom.

## **2. Repositioning of optics using femtosecond lasers induced controlled expansion**

### *2.1 General concept*

To reposition optical elements after packaging so that to compensate for post-assembly misalignment that are inherent to most attachment procedures and assembly operations, one needs to be able to control accurately up to six independent degree-of-freedom (three axis to define the position of the object and three rotations to define its orientation).

To visualize better the problem, let us consider a simple example of an optical fiber being positioned in front of a waveguide. In the laboratory, one would typically use a six-degree-of-freedom positioner (or only five if the orientation of the fiber around its longitudinal axis has no importance). Considering transmission losses related to fiber misalignment, such positioner should achieve sub-micron accuracy to achieve optimal coupling with minimal losses. To achieve this level of accuracy, precision mechanisms like flexures are used, eventually combined with active devices like piezoelectric actuators.

While this works well in a laboratory environment, at the package level, it is much more difficult to accomplish. With some rare exceptions mentioned above – and limited to simple problems, post-assembly realignment is in general, not done due to the lack of a suitable method, capable of addressing the various post-assembly misalignment issues.

A strategy to overcome this limitation and that can potentially open new frontiers in precision assembly is the following. Let us consider a glass substrate as the supporting substrate for the optical elements to be repositioned. This element can be itself machined in a way such that it defines a kinematics structure in addition to holding the optical component or fulfilling itself an optical function. Such complex structure can be entirely manufactured out of fused silica glass and with three-dimensional capability [14–16] using non-ablative femtosecond laser exposure combined with a chemical etching step (either in HF [17] or KOH

[18]). To ‘activate’ this flexural element, one needs a one-time actuation means so that once the desired position is found; the flexure holds its position permanently. To implement this function, we propose to use femtosecond laser induced localized volume expansions. Indeed, in a previous work, we have shown that laser exposure of fused silica in the non-ablative regime induces a net-volume change [19]. This concept of femtosecond laser-assisted repositioning is schematically described in Fig. 1 that considers an illustrative example of optical packaging task: light-coupling in an optical fiber with a given numerical aperture. The fiber core is usually a few microns in diameter. Efficiently coupling light in such waveguide requires sub-micron accuracy in relative positioning.

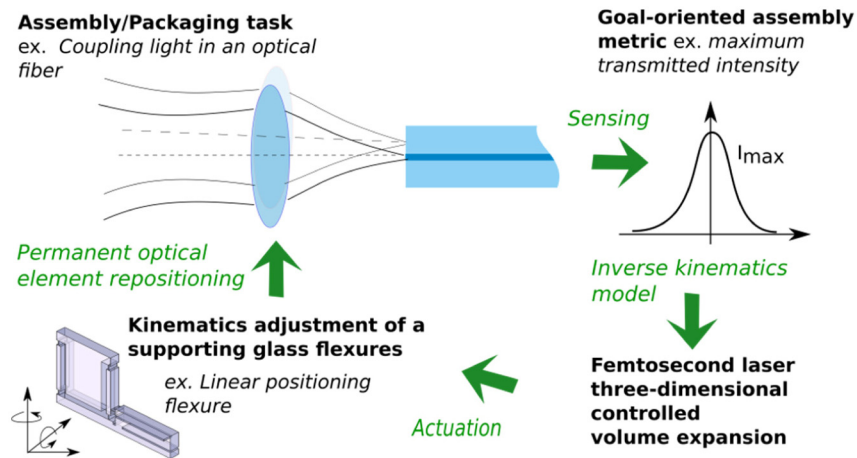


Fig. 1. Illustration of the concept of repositioning through femtosecond laser-controlled volume expansion: we consider a typical assembly task (optical fiber-light coupling) that requires positioning an optical element with respect to another one along up to six axes. In a goal-oriented assembly strategy, a measurable metric is defined to assess the optimal alignment, based on the function of the device, as opposed to defining absolute positioning based on the actual objects dimensions and tolerances. Here, a femtosecond laser is used to permanently deform a glass element forming a positioning flexure kinematics supporting the optical element to be adjusted. Thanks to non-linear absorption, this controlled deformation can be achieved in the three dimensions, making possible the implementation of repositioning tasks according six degrees of freedoms.

Figure 2 shows two examples of controlled deformations that can be induced by locally exposing a glass element. The first case is a cantilever. Exposing the upper part near the surface in a laser exposure regime where nanogratings form will cause the cantilever to bend up [19]. Exposing the lower surface will cause the opposite motion. In a flexure mechanism, bending can be used to mimic the behavior of a classical pivot. The second example illustrates a U-shape element being exposed to the femtosecond laser through its thickness. Laser exposure in this case causes a translation of the free-end of the structure. (This example will be further developed in the next section where a proof-of-concept of repositioning is introduced and analyzed.) These are just two examples to illustrate the concept. Since laser-affected zones can occupy virtually any three dimensional volume inside any given shape, an infinite variety of controlled deformation can be designed to achieve complex motion.

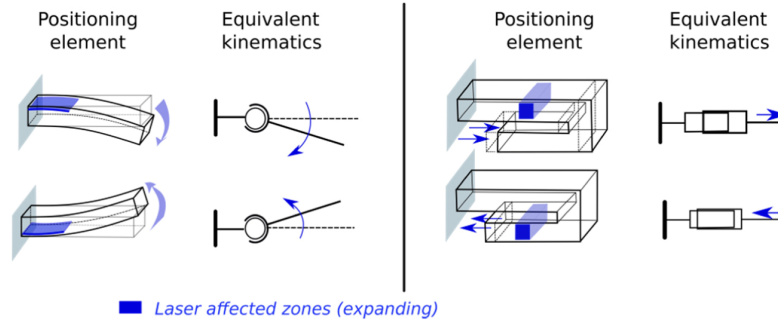


Fig. 2. Examples of rotational and translational fine motions that can be induced by localized femtosecond laser volume exposure (the blue zones in the schematic). The equivalent kinematic is shown next to it. The first two illustrate the example of a beam bending mimicking a pivot joint, while the two others show a linear element that expands or retracts depending on which region is exposed. These are just simple illustrations. Complex displacements can be obtained by exposing more complex volumes and/or using different actuator shapes.

Note that opposite-signed deformation could be induced using different laser exposure conditions, for instance, using short pulse lasers inducing localized densification [20] or volume expansion depending on the chosen pulse energy.

Whatever approaches is taken or whatever repositioning element design is selected, the general principle remains the same that is ‘*using measurable goal-oriented assembly metric or figures of merit, the axis that requires adjustment is locally and iteratively activated until the optimum permanent alignment is obtained*’. Such approach allows for robust correction of manufacturing and assembly tolerances.

Let us now consider a practical implementation of this concept to illustrate its potential. For the sake of demonstration, we consider the case of a one degree-of-freedom proof-of-concept utilizing the U-shape structure presented in Fig. 2 right. As emphasized above, this approach is not limited to a single axis but can be extended to complex geometries.

### 2.2 One degree-of-freedom proof-of-concept

This proof-of-concept considers a one-degree-of-freedom repositioning task. The prototype demonstration for the demonstration is shown in Fig. 3.

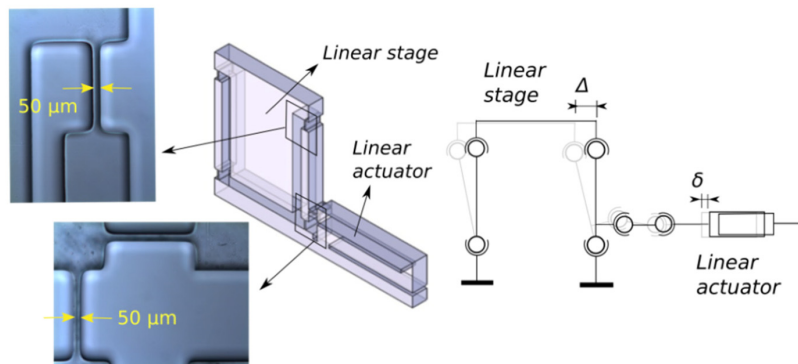


Fig. 3. A computer-assisted drawing (CAD) of a proof-of-concept as well as close-up microscope pictures of a fabricated specimen are shown. This device is a one axis linear flexure stage onto which a U-shape element is connected to. The flexure itself further consists of four notch hinges. The U-shape element, later referred as ‘one-time actuator’ is position so that a small elongation of this element induces a larger displacement of the flexure, through a simple lever mechanism. The equivalent kinematics of this mechanism is illustrated (right side).

This device consists of a one axis linear flexure stage (that would hold an optical function or element) with a U-shape element is connected to. This element will be later on referred as a ‘one-time actuator’. The flexure itself further consists of four notch hinges. The ‘one-time actuator’ is positioned so that a small elongation of this element induces a larger displacement of the flexure. This is a classical design for amplifying the motion of a device. In this particular case, the one-time actuator is connected to the flexure-guidance to induce a ten times amplification at the end of the moving element.

The actuator is operated by exposing scan patterns on either its lower or upper beam. The working principle is further explained in Fig. 4. The basic principle is to make use of the net volume expansion observed when writing laser lines. Using a micro-cantilever method, this net expansion has been demonstrated and quantified in [19]. This net expansion produces anisotropic stresses preferably oriented along the laser polarization axis, as observed in [21,22]. The order of magnitude of this volume expansion varies according to exposure conditions such as pulse energy and energy deposition (or net fluence), but typically is in the order of 0.01 to 0.05%. This volume expansion can also be further tuned by exposing a more or less large volume of matter by juxtaposing laser-written lines, like for instance staking them regularly as illustrated in Fig. 4 with varying spacing parameters. Unlike laser-induced methods based on localized melting or induced plasticity through a sacrificial layer, here the deformation is introduced in the three-dimension, and since it is done through a non-linear absorption process, with accuracies that can be smaller than the laser wavelength itself, therefore sub-microns.

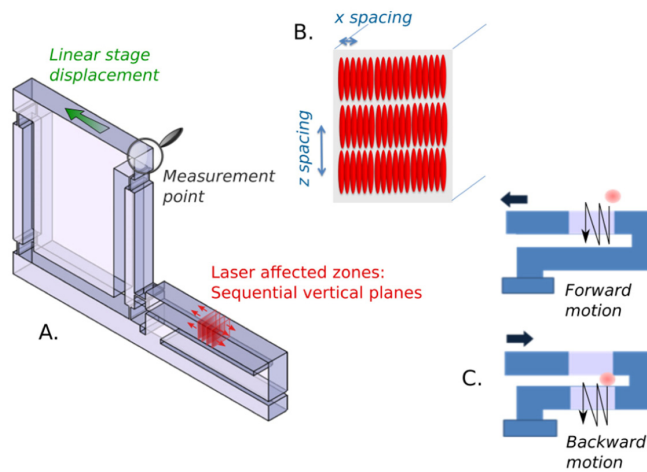


Fig. 4. Linear stage (A) working principle: a laser-pattern consisting of a set of adjacent lines (B) is written across the width of the one-time actuator beam (C), to create uniform elongation along the actuator axis. In this experiment, after writing the pattern, the induced displacement is measured without removing the specimen from the laser platform (measurement point (A)) to ensure high measuring accuracy of the laser-induced displacements.

Interestingly, since these laser-affected zones can be arbitrarily distributed within a given volume (even near sharp edges pending that appropriate beam-shaping techniques are used [23]) and since the laser polarization can further tune the level of stress and orientation of these written lines (as demonstrated in [21,22,24]), virtually any arbitrary stress-state can be created in the material that, if coupled with a specific stiffness matrix, will further induce a prescribe deformation action. For instance, one can think of creating linear, bending or torsional deformation following this principle. Femtosecond laser exposure can therefore be seen as a tool for ‘direct-write deformation state’ in the volume of a transparent material.

### 3. Results and discussion

#### 3.1 Fabrication procedure

The laser exposure consists of exposing a fused silica substrate (high-OH content) to non-ablative femtosecond laser pulses emitted at a frequency of 800 kHz. The pulses are emitted from an Yb-fiber amplified femtosecond laser (Femtoprint prototype, Amplitude Systèmes) at a wavelength of 1030 nm. The measured pulse duration is 270 fs. The beam is focused through an objective with a NA of 0.4 (Thorlabs, OFR objective, LMX-20H-1064). The contour of the structure is exposed by translating the substrate mounted on high-stiffness/high-acceleration direct drive positioning stages (Micos, Ultra-HR) at an average velocity of 10 mm/s. Further details about this manufacturing process can be found in [25].

#### 3.2 Measurement of induced displacements by third-harmonic generation

To avoid displacing the specimen after exposing it to the femtosecond laser, the same laser is used to measure the actual displacement of the moving stage. We use non-linear third-harmonic emission (THG) [26–29] to locate the position of the moving platform and to measure its displacement. Indeed, glass being centrosymmetric, laser THG is emitted (mostly along the optical axis) when the laser beam crosses a glass edges due to the sharp index contrast. It can therefore be used to locate edges and, in our case, to measure the displacement of the linear guidance. A typical measured profile intensity of the emitted THG when crossing the glass while moving along the optical axis is shown in Fig. 5 (profile #1).

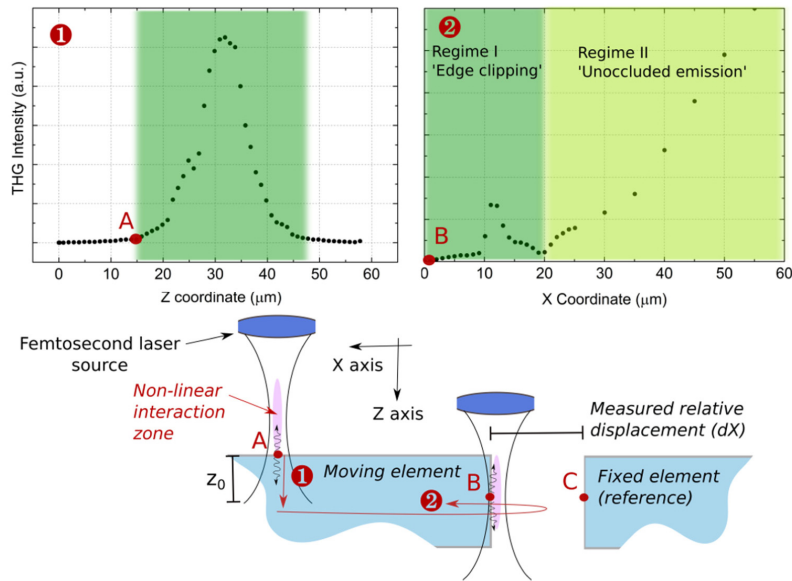


Fig. 5. Top: Typical THG intensity profiles: a) when moving the laser into the surface (#1), b) when moving across a glass edge (#2). Bottom: Strategy use to measure the displacement induced in the flexure. In this example, we measure the displacement of the linear axis. The surface is first precisely located (point A) based on the onset for THG emission. Second, the laser is moved by a fix-amount from point A. Then, the laser is moved inside the structure toward the glass edge. Point B is recorded when THG is detected when moving the laser again into the material. The same procedure is applied for point C. Finally, the measured relative displacement ( $dX$ ) is deduced from the knowledge of points B and C.

This profile is similar to the ones reported before by Barad *et al.* [27] and others [24–27]. A similar profile can be obtained when crossing an interface perpendicular to the optical axis (see Fig. 5, profile #2). In such case, a secondary peak that can be correlated to beam-clipping

effect is observed. This second regime has similar characteristics than for the crossing along the z-axis, but with higher intensity as the non-linear interaction cross-section is larger.

The measurement strategy for accurately measuring the relative displacement of the flexure is the following. We first use the THG z-profile (#1 in Fig. 5) to find a reference point nearby the surface. This point (A in Fig. 5) is identified by the onset of THG. From there, we move in the glass by a fix amount (here 100 microns), and then move toward the glass/air interface, exit and move back again to extract profile #2 in Fig. 5. The observed onset for THG is used to define point B on the moving element. The same procedure is followed to define the fixed reference point C. The relative displacement of the linear stage with respect to a fixed reference is then deduced from the measured points B and C. Note that the fixed point C is re-acquired each time a new measurement is made to increase the repeatability of the procedure. The measured repeatability of the moving stages is less than  $\pm 100$  nm for displacement smaller than 20 mm. Taking into account the cross-section size of THG interaction zone, we estimate the overall repeatability of the measurement to be in the same order.

### 3.2 Results

To validate the concept of femtosecond assisted laser repositioning, four test specimens were exposed with three different laser parameters. In each case, laser written patterns consisted of block of adjacent lines forming a rectangular laser affected zones. Here 200 lines, parallel one to another are written across the volume. The laser polarization is chosen perpendicular to the laser writing direction. In other words, the nanogratings planes are perpendicular to the actuator long axis. Note that, as shown in [19,22], the level of stress depends on the polarization of the laser beam. Therefore, one could use the laser polarization to further tune the amount of stress inserted in the material. For the first two cases, three blocks of lines are written, one next to another.

The results show three different situations, shown in Table 1 and visually in Fig. 6. In the first two cases (#1 and #2), very large, but irregular displacements are achieved. A close examination of the specimens (see Fig. 6) indicates the presence of cracks, or – in case #2, the collapse of the main actuator beam. This formation of cracks is not so surprising and further illustrates the potentially high level of stress introduced between laser written lines. In [21], we estimated the level of stress to be close to one GPa or above. Cracks follow preferably the laser-written lines orientation and therefore, the nanogratings planes.

Table 1 reports on the corresponding displacement measurements. Not surprising, cases #1 and #2 yields rather large displacement but inconsistent as a result of the fracture of the specimens. Cases #3 and #4 illustrates examples where the laser intensity is properly tuned. In this example, the equivalent displacement observed by single line writing varies between 0.1 and 0.2 nm. We attribute the difference of amplitude between the expansion and the contraction mode of the actuator to the stiffness asymmetry of the U-shape actuator. Such effect can easily be compensated for, either by using different laser polarization, pulse intensity or simply changing the line spacing.

**Table 1. Volume expansion and equivalent displacement induced per written line for four different experiments.**

Specimens	Actuator mode	Pulse energy (nJ)	Linear motion amplitude (microns)			Equivalent displacement induced per written line (nanometers)		
			Pattern 1	Pattern 2	Pattern 3	1	2	3
#1	Expands	275	14.25	9.07	28.49	7.125	4.535	14.245
#2	Shrinks	240	9.04	8.2	152.24	4.52	4.1	N.A.
#3	Expands	230	4.39	3.99		0.22	0.20	
#4	Shrinks	230	4.70	5.57		0.12	0.14	

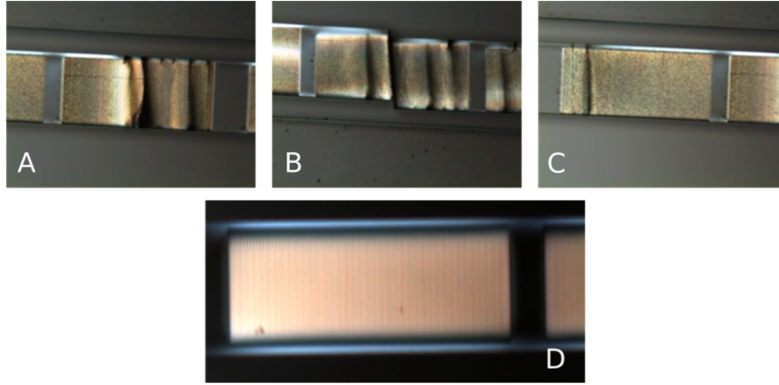


Fig. 6. Microscope close-up view of the actuator for extreme cases (A-C) of over-stressed specimen (cases 1 and 2 in Table 1) and for an homogeneous crack-free loaded specimen (D) seen in cross-polarized image. Cracks are clearly visible (A,C) and in the extreme case (B), the structure collapsed. Cracks are oriented along the laser line written direction.

### 3.3 Photoelastic analysis of the stress state in the device after exposure

The structure being entirely made of silica, one can directly observed the stress-state of the material by observing the stress-induced birefringence in the material. These observations presented in Fig. 7 reveal the stress present in three key locations in the device. Inset 1 in Fig. 7 shows the lower hinge (A) and the hinge (B) connecting the U-shape actuator to the linear stage. As can be seen hinge B sees essentially a quasi-pure bending stress state, characterized by a stress (and therefore, a retardance) maximized on the edges and zero in the middle. Hinge A on the other end sees a mixed loading mode, combining bending and shear stress. The presence of the shear stress can be considered as parasitic and non-productive. This shear stress is due to the proximity of the point load, i.e. where the actuator is connected through hinge B. This is a trade-off. The closer the force application point is to the hinge A, the higher the amplification ratio between the actuator and the end-measuring point, however the higher is the shear stress in the pivot A. Since the hinge C (Inset 2) is far from the force application point, the deformation mode that dominates in this case is a bending mode as expected and as can be verified in the photoelastic image.

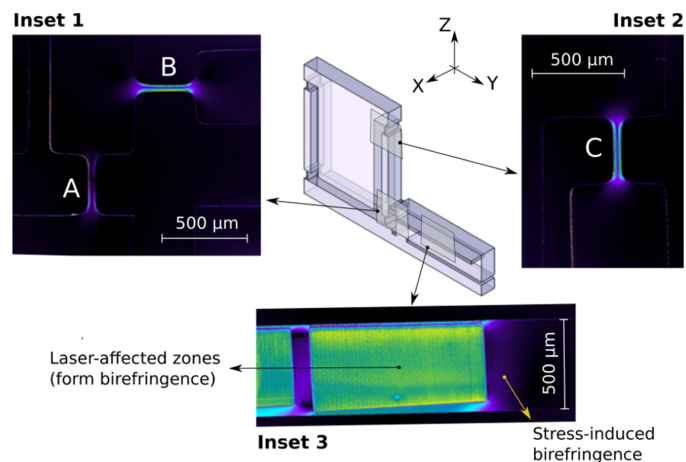


Fig. 7. Photoelastic measurements performed on the test specimens. The photoelastic images were taken from various locations of interest on the specimen. Inset 1 shows the connection between the actuator and the linear stage, inset 2 one of the upper hinge and inset 3 one set of laser-affected zones.

#### 4. Conclusions and perspective

Reliable packaging in optics so that optical alignment is maintained is often a difficult task in particular when high level of accuracy is to be sought. In fact, it is often the bottleneck for transferring and translating optical laboratory demonstrations into reliable and cost-effective products.

In this work, we have demonstrated that femtosecond laser exposure with non-ablative pulses can be used to reposition an element on a substrate. The working principle is to induce localized deformation *in the bulk* of the material to create controlled stress states that can be *channeled* through a dedicated flexure-based kinematics into a macroscopic deformation. As an illustration, an simple example of a single-axis positioning stage being ‘adjusted’ permanently by applying localized laser exposure point on U-shape structure was shown. Using this principle, sub-nanometer displacements were induced.

While the idea of localized deformation of material to compensate for alignment inaccuracies have already been proposed and put in practice for simple case, femtosecond laser brings these concepts to another level, making possible the repositioning in the three-dimensions and with unprecedented resolutions and controlled levels, thanks to the non-linear matter interaction and the very localized deformation induced by the laser.

Combined with appropriate kinematics and design, repositioning can virtually be induced along all six axes defining the position and orientation of an object in space. Combined with the writing of waveguides [31–33], gratings [34,35], flexures [14,15], fluidics channels [25], optical elements [36,37] and resonators [38], the additional capability of laser-assisted fine-adjustment brings femtosecond laser micromachining to a step closer to realizing fully integrated monolithic platform.

#### Acknowledgments

The author thanks the European Research Council (ERC-Stg Galatea, ERC-2012-StG-307442) for supporting this research.